

1 **Vegetation and Habitat Classification of Created and Natural Brackish Marshes**
2 **via Unoccupied Aerial Systems (UAS): A Case Study of the Lake Hermitage Marsh**
3 **Creation Project**

4 Seth T. Chapman^{1*}, Coy LeBlanc², James Nelson^{2,3}, Brian J. Roberts⁴, Michael J. Polito^{1,5}

5 ¹Louisiana State University, Baton Rouge, LA, USA; ORCID: 0009-0000-6952-4150

6 ²University of Louisiana, Lafayette, LA, USA

7 ³Present Address: University of Georgia, Athens, GA, USA

8 ⁴Louisiana Universities Marine Consortium, Chauvin, LA, USA; ORCID: 0000-0002-6366-3165

9 ⁵Present Address: Department of Ocean Sciences, University of California Santa Cruz, Santa
10 Cruz, CA, USA; ORCID: 0000-0001-8639-4431

11

12 *Corresponding author, e-mail address: sethchapman11198@gmail.com

13

14 **ABSTRACT:**

15 Much of Louisiana's coastal wetlands have been lost over the last century, leading to federal
16 and state agencies allocating billions of dollars towards coastal restoration, flood protection,
17 and marsh creation projects. Traditional post-construction monitoring of marshes involves in-
18 situ vegetation sampling and aerial imagery from fixed-wing occupied aircraft, but these
19 methods can be logistically intensive and limited in spatial and temporal resolution. To address
20 these limitations, we evaluated the use of Unoccupied Aerial Systems (UAS) in post-
21 construction monitoring of the Lake Hermitage Marsh Creation Project in Plaquemine Parish,
22 Louisiana as a case study. Specifically, we used UAS-derived habitat classification maps to
23 compare vegetation cover between created and reference (i.e., natural) marsh sites and
24 conducted a power analysis to quantify the number of in-situ plots needed to reliably
25 characterize site-wide vegetation cover. Habitat classification accuracies of UAS-derived maps
26 ranged from 77.9 – 84.5% with slightly lower accuracies at created relative to reference marsh
27 sites due to their more heterogenous vegetation cover. UAS-derived maps discriminated
28 between created and reference marsh sites based on vegetation community similarity, while in-
29 situ vegetation monitoring plots did not. Furthermore, our case study illustrates the ability of
30 UAS-based habitat and vegetation classifications to complement, inform, and optimize plot-
31 based, in-situ vegetation sampling in future post-construction marsh monitoring plans.

32

33 **KEY WORDS:** Coastal monitoring, drones, created wetlands, unoccupied aerial systems, remote
34 sensing

35 **1. INTRODUCTION**

36 Louisiana's coastal wetlands have been disappearing over the last century and will
37 continue to do so unless significant action is taken (Barras et al. 2003). Approximately 5000 km²
38 or 25% of coastal wetland has been lost since the 1930s and another 4500 km² are projected to
39 be lost over the next 50 years (Couvillion et al. 2016). Federal and state agencies have allocated
40 funds to counteract existing coastal land loss and potentially prevent further losses. For
41 example, the Coastal Wetlands, Planning, Protection and Restoration Act (CWPPRA) is federal
42 legislation that supports wetland restoration and funds selected projects (CWPPRA 1990;
43 LCWCRTF 1993). In addition, the Louisiana Coastal Protection and Restoration Authority (CPRA)
44 has developed a Coastal Master Plan that allocates \$50 billion for restoration and risk reduction
45 projects (CPRA 2023). This includes sediment diversions, barrier island restoration, hydrologic
46 restoration, and shoreline protection projects, with the largest funding, \$15 billion, directed
47 towards marsh creation (CPRA 2023).

48 Marsh creation projects commonly uses dredged sediments taken from commercial
49 waterways and places them in project areas where marsh habitats have been previously
50 degraded into open-water systems (CPRA 2023). Post-construction monitoring, including
51 vegetation surveys, is a common component of marsh creation projects which allows managers
52 to assess project success (DWHNRDAT 2017). Post-construction vegetation surveys typically
53 estimate the percent cover of plant taxa in plots along one or multiple transects or distributed
54 in a semi-random fashion. CWPPRA funded projects in Louisiana use an adaptation of the

55 Coastwide Reference Monitoring System's (CRMS) vegetation sampling methods for post-
56 construction monitoring (Folse et al. 2023).

57 For example, the post-construction vegetation monitoring plan for the Lake Hermitage
58 Marsh Creation Project in Plaquemine Parish, Louisiana includes twenty 2 m x 2 m monitoring
59 plots across the 322 hectare CWPPRA project area (Richardi 2016). The number of monitoring
60 plots employed in this project was based on the expectations of the site's topographic,
61 hydrologic, and sediment variability (D. Richardi, pers. comm.). Plot locations were then
62 selected in a semi-random fashion informed by topographic surveys and the monitoring
63 budget's constraints that vegetation sampling be completed within a 1–2-day window (Richardi
64 2016). Vegetation monitoring at the Lake Hermitage Marsh Creation Project is also
65 complemented by aerial imagery captured from fixed-wing aircraft used for vegetation analysis
66 (height and composition estimates) and conducting land/water surveys (Folse et al. 2023).

67 While in situ vegetation sampling is common, it is also time and labor intensive and can
68 result in vegetation knockdown, soil compression, and ponding resulting from sampling
69 collections and vehicle access to site interiors (Christie et al. 2016; Minchinton et al. 2019). In
70 addition, aircraft-based imagery is expensive and electro-optical satellite imagery is often
71 limited by spatial/temporal resolution and cloud cover obstruction which can hamper their use
72 in post-construction monitoring plans (Christie et al. 2016; Pettorelli et al. 2018). These
73 logistical and financial issues can limit the effectiveness of post-construction monitoring plans
74 that rely on these techniques.

75 Unoccupied Aerial Systems (UAS) can potentially overcome many challenges faced by
76 traditional in-situ sampling methods. These platforms enable the gathering of visible spectrum,
77 multi-spectral, or hyper-spectral imagery that can be used to produce highly accurate maps for
78 habitat (wetlands, beaches, sea cliffs) and vegetation (marsh, mangrove, aquatic) monitoring
79 (Barlow, Gilham, and Ibarra Cofrã 2017; Cao et al. 2018; Chabot et al. 2018; Jaud et al. 2019;
80 DiGiacomo et al., 2022; Dronova, 2015). In addition, UAS imagery can function as a
81 supplementary tool alongside in -situ vegetation sampling to inform plot selection and expand
82 site characterization (Anderson and Gaston 2013). For example, researchers have used UAS
83 imagery to quantify marsh vegetation height and above-ground biomass (DiGiacomo et al.
84 2022; Doughty and Cavanaugh 2019), derive land/water area metrics and Normalized
85 Difference Vegetation Indices (NDVI; (C. N. Brooks et al. 2019; Broussard, Suir, and Visser 2018;
86 Sturdvant et al. 2017; Yang et al. 2019)), and evaluate wetland vegetation quality and
87 productivity (Broussard, Visser, and Brooks 2020; Harris 2020). Other studies have applied UAS
88 in coastal erosion, flooding, and storm event assessment both over long timescales and as
89 quick-response data collection (Appeaning Addo et al. 2018; Duo et al. 2018; R. Morgan et al.
90 2022; Morgan et al. 2023). These studies highlight the ability of UAS approaches to quantify
91 habitat characteristics in coastal systems and indicate their potential to inform post-
92 construction vegetation monitoring.

93 The goal of this study is to evaluate the use of UAS platforms for post-construction
94 vegetation monitoring using the Lake Hermitage Marsh Creation Project as a case study. Our
95 study had three specific objectives. First, we used UAS imagery in conjunction with in-situ

96 vegetation data to generate and assess high-resolution habitat and vegetation classification
97 maps. Second, we used a combination of UAS imagery and in situ vegetation plots to compare
98 habitat and vegetation cover between created and reference (i.e., natural) marsh sites. Finally,
99 we used UAS-derived vegetation classification maps to conduct a power analysis that evaluates
100 current monitoring plans at these sites and guide restoration managers in the selection of the
101 appropriate number of monitoring plots needed to reliably characterize site-wide vegetation
102 communities using plot-based sampling. We aim to use the products generated from these
103 efforts to evaluate the implementation of UAS platforms as a complement to in-situ
104 methodologies for large-scale/site-wide vegetation monitoring and to inform existing in-situ
105 methods including transect and plot placement for vegetation monitoring.

106 **2. METHODS**

107 **2.1 Study Area**

108 Our study focused on the Lake Hermitage Marsh Creation Project (BA-42) located along
109 the eastern side of Barataria Bay, in Plaquemine Parish, Louisiana (Fig. 1). This area of Barataria
110 Bay is characterized by brackish marshes with salinity ranging from 8-15 (Chabreck 1970), with
111 vegetation typically dominated by grasses such as *Spartina alterniflora*, *Spartina patens*, or
112 *Distichlus spicata*, rushes such as *Juncus roemarianus*, reed such as *Phragmites australis*, and
113 shrubs, small trees and other woody vegetation such as *Iva frutescens* (Keppeler et al. 2023).

114 The Lake Hermitage Marsh Creation Project constructed ~322 hectares of land using
115 hydraulically dredged Mississippi River sediments (Richardi 2016) with support from the Coastal

116 Wetlands Planning, Protection and Restoration Act (CWPPRA) between 2012 and 215 (Fig. 1).
117 An additional ~42 acres of marsh area was created using excess dredged materials with Natural
118 Resource Damage Assessment (NRDA) support (DHNMP 2015). We examined two created and
119 two reference (i.e., natural) marsh sites in and adjacent to the project area for this study. We
120 sampled created marsh sites within two of the project's primary fill areas in this study: Marsh
121 Creation Areas A and B, referred to hereafter as Lake Hermitage A (LHA) and Lake Hermitage B
122 (LHB; Fig. 1). LHA was constructed from August 2012 to October 2013 and was approximately
123 8.5 years old at the time of this study, and LHB was constructed between December 2013 to
124 May 2014 and was approximately 8 years old at the time of this study. Due to logistical
125 constraints, only the western half of LHA was surveyed in this study (Fig. 1). In addition, we
126 sampled two reference marshes adjacent to the Lake Hermitage Marsh Creation Project: Lake
127 Hermitage Control (LHC) and the Coastwide Reference Monitoring System (CRMS) site CRMS-
128 3680 (Fig. 1).

129 **2.2 Imagery Collection**

130 Imagery used in this study was collected on a single day May 3, 2022, between 10:00. –
131 17:00 CST, using a Trinity F90+ fixed-wing UAS equipped with a MicaSense RedEdge-MX Dual
132 camera system (Fig. 2). Conditions during the image collection were sunny with occasional
133 clouds with mild winds. This fixed-wing UAS is noteworthy for its vertical takeoff and landing
134 capabilities while being a fixed-wing UAS, its integrated autopilot system, long flight times (90+
135 minutes), and high wind tolerance during flights (12 m/s). The MicaSense RedEdge-MX Dual
136 camera system integrates two five-band sensors as well as a Downwelling Light Sensor to

137 output 10 reflectance bands: coastal blue at 444 nm, blue at 475 nm, green at 531 and 560 nm,
138 red at 650 and 668 nm, red edge at 705, 717, and 740 nm, and near-infrared at 842 nm. Facing
139 downward, the sensor's maximum field of view was 34.5 degrees. The drone platform includes
140 an internal GNSS receiver that communicated with the closest available reference station to
141 produce georeferenced imagery with 8 mm horizontal RMS and 15 mm vertical RMS.

142 We planned flights using the Quantum Systems QBase 3D mission planning software
143 (Fig. 2). Flights were conducted at ~122 m altitude, the U.S. Federal Aviation Administration's
144 legal high limit for small UAS operations, to output high resolution imagery while maximizing
145 area coverage. Side and front overlap of the imagery ranged from 70 – 75 percent on each of
146 the sites and flight speed was variable as the UAS compensates for changes in wind speed.
147 Flight times over our selected sites ranged from 50 – 90 minutes totaling flight time for this
148 study at ~5 hours. These parameters allowed for < 8.4 cm pixel resolution in the final maps used
149 in this study.

150 **2.3 Imagery Processing**

151 Imagery obtained during UAS flights was mosaicked within the Pix4D Mapper software
152 to create orthomosaics and 3D digital surface models (DSMs) using Structure from Motion
153 (SfM) algorithms. Orthomosaics are high-resolution, georeferenced photo representations of a
154 ground area generated from, in this study's case, 4500 to 15000 images per site (Fig. 2). Digital
155 Surface Models are digital elevation models that represent the tallest point of surfaces and
156 objects such as vegetation. The SfM technique to generate surface models provides an

157 affordable yet effective alternative to producing elevation data compared to LiDAR (Forsmoo et
158 al. 2019).

159 Pix4D evaluated imagery metadata to determine the image coordinate system, altitude,
160 and location details for each picture. The coordinate system for output orthomosaics was NAD
161 1983 StatePlane Louisiana South FIPS 1702 (US Feet). Image scale used for processing was one
162 half. A maximum number of five images were used per manual tie point and orthomosaics were
163 generated with 10000 keypoints (Fig. 2). Processing was performed on a computer with 128 GB
164 of RAM, an Intel Xeon CPU E5-1603 v3 @ 2.80GHz, and an NVIDIA GeForce RTX 2080 Ti GPU.

165 **2.4 Object-Based Imagery Analysis (OBIA)**

166 We used an object-based image analysis method to perform vegetation analysis of our
167 sites using eCognition Developer v 10.3 (Trimble Inc. 2023; Fig. 2). Orthomosaics and Digital
168 Surface Models (DSMs) output from Pix4D were uploaded into eCognition for each site and
169 provided 11 layers for use in imagery analysis: two blue, two red, two green, one near-infrared,
170 three red-edge, and one elevation surface model bands. Using these 11 available layers, we
171 performed a multi-stage image segmentation to group pixels together into larger distinct image
172 “objects” (Dronova 2015).

173 From these created objects, we developed an object classifier to distinguish among
174 habitat classes at each site (Fig. 2). Habitat classes included water and four terrestrial
175 vegetation types. Water was chosen as it is both spectrally and functionally distinct from
176 terrestrial habitat classes (Broussard, Suir, and Visser 2018) and the four terrestrial feature

177 classes were selected to best characterize the dominant vegetation at each site. First, a “reeds”
178 class, reflecting the dominance of *Phragmites australis*. This species occurs in tall (1-6 m), dense
179 stands and stabilizes marsh platform due to its extensive root systems (Knight et al. 2018).
180 Second, a “shrubs/trees” class, reflecting a dominance of woody vegetation that is visually
181 distinct from the herbaceous species present on these sites. Third, a “grasses” class reflecting a
182 combination of the three dominant marsh grass species found on these sites - *Spartina*
183 *alterniflora*, *Spartina patens*, and *Distichlus spicata*. Some prior studies using aerial imagery
184 have had success in classifying *S. alterniflora* separately from *S. patens* and *D. spicata* (Harris
185 2020), as *S. alterniflora* is functionally distinct (food source, habitat, biogeochemistry) from *S.*
186 *patens* and *D. spicata*, while others have not (Correll et al. 2019). We chose to group these
187 three taxa into a single class in this study as a preliminary analysis indicated that on these four
188 sites senesced patches of *S. alterniflora* had broadly similar spectral characteristics relative to *S.*
189 *patens* and *D. spicata* making distinct classification among these grasses beyond the capacity of
190 this project. Fourth, a “rushes” class reflecting a dominance of *Juncus roemarianus* which occur
191 on these sites as tightly packed, spiky, dark green patches.

192 We adopted a fully supervised method to configure our object classifier, starting by
193 choosing a set of known objects from each habitat/vegetation category (such as water, reeds,
194 shrubs/trees, grasses, and rushes) at every site. We used these selected objects to determine
195 which features (reflectance bands, elevation, brightness, NDVI, etc.) were most effective at
196 distinguishing our specified habitat/vegetation classes, detailed further in our Supplementary
197 Methodology. This approach allowed us to tailor the object features for each site, which were

198 then applied to classify objects into the five predetermined habitat/vegetation classes at each
199 location using eCognition, as documented in Supplementary Tables 1-5. Finally, the fully
200 classified habitat/vegetation maps for each site were exported from eCognition for additional
201 analysis.

202 **2.5 Classification Accuracy Analysis**

203 We conducted an accuracy assessment based on a comparison of the classified maps
204 and base imagery at select points within each site using a stratified random approach in ArcGIS
205 Pro (Congalton 1988). Accuracy assessment points at each site were standardized to three
206 points per hectare of site area or a minimum of 50 points per site whichever was larger. The
207 classification of accuracy points was compared to site orthomosaics to create an Error Matrix
208 that contained the Producer's, User's, and Total accuracies of each site. Producer's accuracy
209 assesses errors of omission made by the classification map (i.e., a measure of false negatives).
210 An example of an error of omission is when a point on the base imagery is water, but the
211 classification map misclassified the point as reeds. User's accuracy assesses errors of
212 commission made by the classification map (i.e., a measure of false positives). An example of an
213 error of commission is when the classification map says a point is water, but the base imagery
214 shows it as reeds. Total accuracy describes how often the accuracy points were correctly
215 classified across all habitat classes by a classification map. The Kappa coefficient was also
216 calculated at each site. This is a statistical evaluation of the accuracy of a classification that can
217 range from -1 to 1, with values near -1 being worse than randomly assigned classifications, 0

218 being no better than randomly assigned classifications, and values near 1 being significantly
219 better.

220 **2.6 In Situ Vegetation Sampling**

221 The post-construction vegetation monitoring plan for the Lake Hermitage Marsh
222 Creation Project includes 20 sampling plots that was last sampled in 2018 and will be sampled
223 again in 2025 and 2034 (Richardi 2016). This includes 4 plots at LHB and 2 plots in the western
224 portion of LHA surveyed in this study. Given the timing between the last vegetation survey
225 (2018) and this study (2022), and because the monitoring plan does not include plots at the LHC
226 reference marsh site, we conducted independent vegetation sampling at the three Lake
227 Hermitage sites (LHA, LHB, and LHC) on May 12, 2022. Aboveground vegetation (clipped at the
228 sediment surface) was collected from replicate (1 m apart) 0.25m x 0.25m plots at five
229 distances (1, 10, 25, 50, and 100 m) from the marsh edge along a transect at each site. The
230 vegetation was sorted by species, and rinsed free of sediment and epiphytes, and then dried to
231 constant mass at 70°C to determine aerial aboveground biomass (in grams) by species for each
232 quadrat (Hill and Roberts 2017).

233 Vegetation sampling data from one additional reference marsh, CRMS-3680, was
234 retrieved from the Coastal Information Management System (CIMS) database
235 (<http://cims.coastal.louisiana.gov>). CRMS site sampling occurs between August 1 and
236 September 30 (end of growing season) of each year and is conducted along a 282.8-m transect
237 at ten 2 m x 2 m vegetation plots. CRMS-3680 was sampled on July 28, 2022. Specifically, we
238 retrieved data on the percent cover of vegetative species for each plot collected using visual

239 estimates. Aboveground biomass (LHA, LHB, LHC) and percent cover (CRMS-3680) data was
240 then used to identify the dominant vegetation type found in each sampled plot.

241 **2.7 Created vs. Reference Marsh Sites**

242 As a secondary accuracy assessment, we compared the vegetation classes predicted by
243 UAS-classified maps (such as trees/shrubs, reeds, rushes, or grasses) against the dominant
244 vegetation types actually observed in the in-situ vegetation plots sampled at each site. This
245 comparison enabled us to verify whether the dominant vegetation predicted by UAS maps
246 aligned with what was physically observed in each sample plot. Additionally, this process
247 provided a measure of how accurately our maps reflected the real-world conditions of both
248 created and reference sites, in relation to direct, on-the-ground observations. Next, we
249 assessed the similarity of vegetation communities between created and reference sites by
250 creating Bray–Curtis resemblance matrices using the vegan package in R (Oksanen et al., 2018).
251 We created two resemblance matrices: one using classified UAS map data and a second using in
252 situ plot data. To allow for direct comparisons between methods we used percent vegetation
253 class data (i.e., reeds, shrubs/trees, grasses, and rushes) to create both UAS and in-situ
254 resemblance matrices and square-root transformed percentage data prior to analyses. To visualize
255 similarity among created and reference marshes, we then calculated the centroids for each site
256 and constructed separate hierarchical clustering dendrograms using ward.D's algorithm
257 (Murtagh & Legendre, 2014). These dendrograms were then cut into two clusters based on
258 calculated similarity to assess the degree to which UAS classified maps and in-situ plot data
259 identified differences in vegetation communities between created and reference marshes.

260 **2.8 Power Analysis**

261 We used UAS-derived vegetation classification maps to conduct a power analysis to
262 evaluate the degree to which the current, plot-based vegetation monitoring efforts at our
263 sampling sites are representative and identify the required sampling intensity (i.e., number of
264 monitoring plots) needed to reliably characterize site-wide vegetation. We used a probabilistic
265 approach to our power analysis, by generating between 1 to 200 random points (i.e. vegetation
266 plots) within each marsh site's terrestrial area without replacement, iterated 1000 times per
267 number of plots at each site. Randomly generated plots were structured to be no closer than 2
268 meters together to simulate the average size of CRMS vegetation plots (2 m x 2 m). We then
269 assigned a dominant vegetation class (i.e., reeds, shrubs/trees, grasses, and rushes) to each
270 randomly generated plot using the UAS-derived vegetation classification maps from each site
271 and calculated the proportional occurrence of each vegetation class for each iteration. We then
272 calculated the percentage of iterations that resulted in predicted proportional occurrence of
273 the four vegetation classes that fell within 10% of the actual site-wide vegetation cover seen in
274 the UAS-derived vegetation classification maps.

275 We then used binomial regressions between the number of sample plots (1-200) and
276 the probability of the resulting predicted proportional occurrence falling within 10% of the
277 actual site-wide vegetation cover. The resulting statistical relationship allowed us to evaluate
278 the reliability of current monitoring plans at three of our sites by calculating the probability that
279 plot-based sampling accurately reflects site-wide vegetation cover given the 2, 4, and 10
280 vegetation monitoring plots currently in place at sites LHA, LHB, and CRMS-3680 respectively. In

281 addition, we also used this relationship to assess the expected degree reliability if plot-based
282 sampling at LHA and LHB was increased to 10 plots per site similar to CRMS-3680 and other
283 CRMS monitored sites. Finally, we calculated the minimum number of vegetation plots needed
284 to reliably characterize site-wide vegetation at each site by determining when the 95%
285 confidence interval around each binomial regression lines overlapped with 100% (i.e., the
286 number of plots needed for the predicted proportional occurrence of each vegetation class to
287 consistently fall within 10% of the actual site-wide values).

288 **3. RESULTS**

289 **3.1 Habitat Classifications**

290 Total landscape area for the sites ranged from 5.7 to 83.3 hectares (CRMS-3680 and LHB
291 respectively; Table 1). The proportion of total landscape area that was land ranged between
292 69.0 – 77.8% (Table 1). The created sites generally had higher proportions of land area than our
293 reference sites (Table 1). Classified maps indicated that the terrestrial habitat of the four study
294 sites were dominated by the grasses class at all four sites (Table 2; Fig. 3; Fig. 4). The
295 percentage of terrestrial habitat classified (i.e., excluding area classified as water) as grasses
296 ranged from a low of 74.6% at LHB to a high of 97.6% coverage at CRMS-3680. Rushes
297 comprised the second most abundant class at three of the sites (LHA, LHC, and CRMS-3680)
298 with Reeds being the second most abundant at the final site (LHB). Shrubs/trees abundance
299 ranged from 2.5% at LHA to 7.2% at LHB and were not present on the classification maps of LHC
300 and CRMS-3680.

301 **3.2 Classification Accuracy**

302 Producer's Accuracy, a measure of false negatives, ranged from 44.1% to 100% across
303 taxa and sites (Table 2), averaging $78.0 \pm 15.3\%$. Producer's Accuracy averaged slightly lower
304 across all habitat classes at the two created marsh sites (LHA: $73.5 \pm 18.2\%$; LHB: $68.6 \pm 15.6\%$.)
305 relative to the two reference marsh sites (LHC: $82.6 \pm 6.4\%$; CRMS-3680: $83.7 \pm 18.5\%$). User's
306 Accuracy, a measure of false positives, ranged from 54.8% to 100% across taxa and sites (Table
307 2), averaging $78.6 \pm 14.1\%$. User's Accuracy averaged slightly lower cross all habitat classes at
308 the two created marsh sites (LHA: $79.3 \pm 12.7\%$; LHB: $72.6 \pm 15.5\%$) relative to the two
309 reference marsh sites (LHC: $81.0 \pm 16.4\%$; CRMS-3680: $84.1 \pm 15.1\%$). Total Accuracy ranged
310 from 77.9 – 84.5% across taxa and sites (Table 2), averaging $81.2 \pm 3.2\%$. Kappa values,
311 measures showing how well a classification performed against random assignment, were 0.65,
312 0.68, 0.76, and 0.74 at sites LHA, LHB, LHC, and CRMS-3680 respectively. Total accuracies and
313 Kappa values averaged slightly lower at the two created marsh sites relative to the two
314 reference marsh sites.

315 **3.3 In-situ Vegetation Sampling**

316 Grasses were the dominant vegetation class recorded during in situ vegetation sampling
317 at all four sites, ranging from 63 to 98% of plot biomass (LHA, LHC, and LHB) or cover (CRMS-
318 3680; Fig. 4). Four grass taxa were recorded in plots including: *Distichlis spicata*, *Paspalum* sp.,
319 *Spartina alterniflora*, and *Spartina patens*. *Spartina alterniflora* comprised the highest
320 percentage of plots by biomass at LHA (35.6%), LHB (44.4%), and LHC (35.8%) and *Spartina*
321 *patens* comprised the highest percentage of plots by coverage at CRMS-3680 (32.3%; Fig. 4).

322 Rushes, predominately *Juncus roemerianus* but also *Schoenoplectus spp.* and *Bolboschoenus*
323 *robustus*, were the second most abundant vegetation class, ranging from 2 to 33% by biomass
324 (LHA, LHC, and LHB) or cover (CRMS-3860; Fig. 4). Shrub/tree (*Iva frutescens*) and reed (*Typha*
325 *latifolia* and *Phragmites australis*) species were present in low abundance in LHA plots only,
326 with 7% and 3% of total plot biomass, respectively (Fig. 4). Shrubs/trees were observed in areas
327 outside of plots at LHB (but not LHC and CRMS-3860), and reeds were observed in areas outside
328 of plots at both LHB and LHC (but not CRMS-3860). Other herbaceous plant species observed in
329 plots at low abundance (<2% by biomass or cover) include *Cynanchum angustifolium*, *Ipomea*
330 *sp.*, *Lythrum salicaria*, *Solidago sempervirens*, and *Symphyotrichum tenuifolium* (Fig. 4).

331 **3.4 Created vs. Reference Marshes**

332 At the two created marsh sites (LHA and LHB) the predicted dominant vegetation from
333 UAS classified maps agreed with the observed dominant vegetation on the ground in four out
334 of five plots (80%) at each site. We obtained a similar result, with agreement in 8 out of 10 plots
335 (80%) at the CRMS-3680 reference marsh site, while 100% of plots (four out of four) were in
336 agreement at the LHC reference marsh site. Three of the incorrectly classified in-situ vegetation
337 plots were misclassified as the Grasses class, when in situ sampling indicated these plots were
338 dominated by Rushes. In addition, one incorrectly classified vegetation plot at CRMS-3680 was
339 classified as Grasses when in situ sampling noted that this plot was shallow water just adjacent
340 to the vegetated marsh edge.

341 The comparison of vegetation community patterns showed distinct differences between
342 UAS-derived data and field plot observations at the vegetation class level. Specifically, a

343 dendrogram based on UAS-derived data revealed two primary clusters that separated the
344 created marsh sites (LHA and LHB) from the reference sites (LHC and CRMS-3680; Fig. 5). This
345 separation was primarily due to the higher presence of Reeds and Shrubs/trees in the UAS-
346 classified maps at LHA and LHB, in contrast to the reference sites where these vegetation
347 classes were either significantly less common or completely absent (Fig. 4). On the other hand,
348 a dendrogram based on in-situ plot data grouped the sites into two clusters without
349 distinguishing between created and reference marshes: one cluster included LHC, and the other
350 combined LHA, LHB, and CRMS-3680 (Fig. 5).

351 **3.5 Power Analysis**

352 At the three marsh sites with existing monitoring plans our regression model indicated
353 that their current levels of monitoring predicted a 50.6% (LHA: 2 plots), 51.5% (LHB: 4 plots),
354 and 99.9% (CRMS-3680: 10 plots) chance of the resulting vegetation cover estimates being
355 within 10% of the actual site-wide vegetation cover, respectively (Fig. 6). If our three Lake
356 Hermitage marsh sites (LHA, LHB, and, LHC) had monitoring efforts similar to CRMS-3680 and
357 other CRMS stations (i.e., 10 plots per site) our regression model predicted that it would result
358 in a 59.9%, 57.9%, and 89.3% chance of the resulting vegetation cover estimates being within
359 10% of the actual site-wide vegetation cover (Fig. 6). Finally, our regression models predicted
360 that it would require 70, 79, 108, and 31 in situ plots at sites LHA, LHB, LHC, and CRMS-3680,
361 respectively to provide vegetation cover estimates that would consistently (i.e. 100% of
362 iterations) be within 10% of the actual site-wide vegetation cover (Fig 6).

363 **4. DISCUSSION AND CONCLUSIONS**

364 Our case study highlights the utility of UAS-based imagery for post-construction
365 monitoring of coastal marsh restoration projects. Habitat classification map accuracies were
366 slightly higher on the two reference sites relative to the two created sites and both UAS-based
367 and in situ plot sampling identified greater habitat and vegetation heterogeneity at the created
368 marsh sites. In addition, UAS-derived data discriminated between created and reference marsh
369 sites based on vegetation class community similarity, while in-situ plot data did not likely due to
370 differences in the innate spatial scales of the two sampling methods. The greater habitat and
371 vegetation heterogeneity seen at created sites led to their slightly lower UAS classification
372 accuracies and higher number of in situ plots needed to reliably characterize site-wide
373 vegetation cover as predicted by our power analysis. In addition, our power analysis also
374 indicates that all four sites examined in our study sites require increased sampling effort (i.e., a
375 higher number of in situ plots per site) than what is currently implemented for these
376 monitoring plans to consistently (i.e. 100% of the time) provide vegetation cover estimates that
377 are within 10% of the actual site-wide vegetation cover at each site.

378 **4.1 UAS-based Habitat and Vegetation Classification**

379 The generation of accurate habitat and vegetation classifications using UAS-based
380 imagery can be challenging in heterogeneous environments such as coastal marshes. Even so,
381 classification total accuracies in our study ranged from 77.9 – 84.5% which is similar to the
382 levels of classification accuracy observed in several prior UAS-based studies in coastal regions
383 (C. Brooks et al. 2022; Broussard, Visser, and Brooks 2020; Cao et al. 2018; Harris 2020). In
384 these prior studies and ours, homogenous marsh sites were more easily/accurately classified

385 compared to heterogeneous sites (Broussard, Visser, and Brooks 2020; Harris 2020). However,
386 while the created sites in our study were more heterogeneous and difficult to classify relative to
387 reference sites, the created sites studied by Harris (2020) were more homogenous and easier to
388 classify than adjacent reference sites.

389 Our study encountered some of the challenges reported by other UAS-based marsh and
390 coastal system studies (DiGiacomo et al. 2022; Dronova 2015; Manfreda et al. 2018). For
391 example, our study required site-specific habitat classification algorithms due to differences in
392 spectral baselines between sites that were likely due in part to differences in time of day when
393 imagery was collected. Prior studies have also found that the OBIA methodologies we used in
394 our study can be limited by their site-specificity and often require trial and error when
395 parametrizing classifiers to tailor them for sites (Dronova 2015). In addition, prior studies have
396 noted how the use of DSMs in UAS-based habitat classifications can be heavily affected by
397 variable ground elevations (DiGiacomo et al. 2022; Manfreda et al. 2018). Ground elevation
398 survey conducted by a prior study at the three Lake Hermitages sites indicates much more
399 variable average ground elevations at the two created sites (LHA: 0.18 ± 0.13 m; LHB: $0.07 \pm$
400 0.11 m) relative to the reference site (LHC: 0.09 ± 0.04 m; Keppeler et al. 2023). The more
401 variable ground elevation may have led to greater misclassification of tall vegetation classes
402 such as Reeds and Shrubs/trees which relied on DSMs for classification. We found that the
403 presences of senesced *S. alterniflora* at our sites with similar spectral similarity to other
404 vegetation types prevented our ability to classify specific grass taxa and likely contributed to
405 the lower classification accuracies obtained for Rushes. In addition, *Phragmites australis*, the

406 dominant plant within our Reeds category, was undergoing a die-back period on our sites at the
407 time of image collection, creating large spectral value overlap with senesced marsh grasses and
408 leading to a reliance on DSM values for distinguishing between the two classes. Doughty and
409 Cavanaugh (2019) employed the use of a handheld spectrometer during their in-situ vegetation
410 sampling to measure canopy reflectance and inform their later UAS classification. In retrospect,
411 we find that this method could have improved our classification parameters by providing
412 expected spectral values for each target class and recommend implementing the method in
413 future monitoring efforts if within logistical constraints.

414 Our case study also highlights several of the logistical benefits related to the application
415 of UAS coastal marsh monitoring. First, this technology allows for mostly noninvasive
416 monitoring compared to traditional in-situ methodology as exemplified in our study where the
417 only site impact from our UAS collection occurred at the edge of the sites where our boat was
418 moored (DiGiacomo et al. 2022; Manfreda et al. 2018). In addition, we were able to collect
419 aerial imagery for ~170 hectares of marsh in a single day of flights. This demonstrates the
420 potential for UAS-based imagery to expand the spatial coverage of monitoring projects in a
421 manner that is not logically feasible using solely in-situ methods. However, while time
422 efficient in the field, collecting imagery over a single day was likely a contributing factor for the
423 need for site-specific habitat classification algorithms due to differences in spectral baselines
424 between sites. While the framework for UAS analysis applied in our case study (i.e., imagery
425 collection, processing, and classification algorithm development) can serve as a model, future
426 studies will need to similarly balance the likely tradeoffs between rapid (e.g., flights conducted

427 throughout the day) vs. systematic (e.g., flights conducted at consistent times and conditions)
428 imagery collection.

429 **4.2 Created vs. Reference Marsh Vegetation Communities**

430 Marsh restoration is enacted in the attempt to return systems to their original states
431 prior to environmental impacts. Our study is not the first to assess if vegetation communities
432 within the Lake Hermitage Marsh Creation Project are similar to those found in nearby
433 reference marshes. Keppeler et al. (2023) performed a comprehensive analysis of vegetation
434 communities at six marsh sites, including LHA, LHB, and LHC, in 2018 using in-situ, plot-based
435 sampling. They reported these three sites as each being dominated first by marsh grasses
436 followed by rushes. Using Bray–Curtis resemblance matrices and hierarchical clustering of
437 biomass data at the species level Keppeler et al. (2023) also found that vegetation communities
438 varied among marshes. Specifically, the created marsh site LHB clustering with three of
439 reference marsh sites and differed from created marsh site LHA and reference marsh site LHC
440 which clustered together.

441 Our UAS and in situ-based vegetation class data agree with Keppeler et al.'s (2023)
442 findings in that LHA, LHB, and LHC were primarily dominated by marsh grasses followed by
443 rushes. However, the results of our vegetation community similarity analyses differed from
444 Keppeler et al.'s (2023) as well differing between our two data sources (i.e., UAS and in-situ
445 plots). Specifically, UAS-derived data clustered our two created marshes (LHA and LHB)
446 together as being different from the two reference marshes (LHC and CRMS-3680) which

447 clustered together. In contrast, in-situ-derived data clustered LHA, LHB and CRMS-3680
448 together as having similar vegetation communities that differed from LHC. These contrasting
449 results may be attributable to the inherent strengths and biases of each method. For example,
450 UAS-derived vegetation data provides site-wide coverage but can be limited to estimating
451 percent coverage of the dominant vegetation at lower taxonomic resolution. In contrast, in-situ
452 derived vegetation data provides higher taxonomic resolution within the plot area but may not
453 accurately reflect site-wide vegetation cover due to sampling biases related to the number and
454 placement of plots. For example, the in-situ vegetation plots employed by Keppeler et al.'s
455 (2023) and our case study were taken within 100 m of the edge of the sites, limiting the
456 likelihood of data from these plots reflecting vegetation communities found within the interior
457 of each site. Even so, there are past studies that have successfully used UAS for vegetation
458 mapping with higher taxonomic resolution, especially where projects were targeting a specific
459 species of vegetation. The efforts of Brooks et al. (2022) highlight their ability to classify
460 Eurasian Watermilfoil separately from other submerged vegetation in the Great Lakes primarily
461 due to significant spectral differences among their vegetation species. A separate study
462 conducted along the banks of Lake Erie was able to accurately map *Phragmites australis* in the
463 efforts to control the plant's presence as an invasive species wherein they highlight NDVI and a
464 canopy height model being features useful in separating *Phragmites* from other vegetation
465 (Abeyasinghe et al. 2019).

466 **4.3 Power Analysis of Plot-Based Sampling**

467 Plot sampling is a common vegetation monitoring method. However, care should be
468 taken when designing monitoring studies to ensure that the number and/or size of plots
469 employed can reliably characterize vegetation communities and/or detect change within or
470 between sites over time (Hao et al. 2021; Hoffmann et al. 2019; James-Pirri, Roman, and
471 Heltshe 2007; Steyer et al. 2003). For example, James-Pirri et al. (2007) conducted a power
472 analysis to determine the number of 1m² plots needed for in-situ monitoring vegetation
473 community change in New England salt marshes. They found that 20 plots were required to
474 detect subtle changes over time, though in some cases between 5 to 15 plots were adequate to
475 detect major shifts in vegetation communities.

476 In our study, we sought to evaluate the ability of the current, plot-based vegetation
477 monitoring plan at the Lake Hermitage Mash Creation Project and adjacent reference sites to
478 characterize site-wide vegetation cover. The monitoring plan employed within this CWPPRA
479 project is heavily based on the methods used at CRMS sites (Folse et al. 2023) as the goal of
480 CRMS is to provide a network of regularly monitored reference sites that can be compared to
481 CWPPRA restoration projects (Steyer et al. 2003). Past power analyses of CRMS have focused
482 on the number and distribution of reference sites required to identify trends in vegetation
483 communities across coastal Louisiana (Steyer et al. 2003). However, to our knowledge no prior
484 study has assessed the number of plots required to accurately reflect site-wide vegetation
485 cover within CRMS or CWPPRA marsh sites.

486 Our analysis suggests that the current number of monitoring plots at Lake Hermitage
487 Marsh Creation Project sites LHB (4) and the portion of LHA surveyed here (2) are insufficient to

488 reflect site-wide vegetation cover. Specifically, we found that approximately 50% of the time
489 the current level of plot sampling at these two sites is likely to result in estimates that fall
490 outside 10% of the actual site-wide vegetation cover. In contrast, the current number of
491 monitoring plots at CRMS-3680 (10) is 99.9% likely to result in estimates that fall within 10% of
492 the actual site-wide vegetation cover. Furthermore, our results indicate the effort needed to
493 reliably characterize site-wide vegetation cover using plot-based sampling is site dependent,
494 with larger more heterogenous sites (e.g., LHA and LHB) requiring a higher number of
495 monitoring plots than smaller more homogeneous sites (e.g., CRMS-3680). Our conclusions
496 support the recommendation made by prior researchers who suggests that heterogeneous sites
497 require more accuracy sampling points than homogenous sites for statistically valid
498 assessments to be performed (Congalton and Green 2019).

499 We also found that the predicted number of sampling plots needed to reliably
500 characterize site-wide vegetation cover at our four study sites (31-108 plots per site) is well
501 outside of what would be likely logistically or financially feasible for CRMS or CWPPRA projects.
502 As such, UAS-based vegetation surveys represent a more effective and cost-efficient method
503 for characterization of site-wide vegetation cover at these sites. However, it is important to
504 note that the primary goal of plot-based vegetation monitoring at CRMS sites and CWPPRA
505 projects is not site-wide vegetation assessment *per se*, instead it is to generate floristic quality
506 and productivity indices that can be used to track changes in vegetation assemblage over time
507 associated with either natural variation (i.e., CRMS sites) or restoration activities (i.e., CWPPRA
508 projects; Cretini et al. 2011). Furthermore, it is important to recognize that the UAS-based

509 analysis employed in our case study only identifies the single dominant vegetation class in a
510 discrete area, and not the relative cover of multiple vegetation taxa within plots as in-situ
511 sampling. Even so, our results suggest the potential for the indices and trends derived from in-
512 situ plots at CRMS sites and CWPPRA projects to not necessarily be reflective of site-wide
513 vegetation conditions. Given the differing spatial and taxonomic resolutions, using UAS and
514 plot-based methods in combination is likely to provide a more accurate and comprehensive
515 assessment view of vegetation communities than either method can provide in isolation. As
516 such, we recommend that restoration managers in Louisiana embrace the potential for UAS-
517 based surveys to optimize the number and placement of monitoring plots at CWPPRA and
518 CRMS sites to ensure they are reflective of the vegetation communities present, similar to how
519 UAS-based approaches have been integrated into studies of other systems (Hao et al. 2021;
520 Hoffmann et al. 2019).

521 **4.4 Conclusions and Recommendations**

522 This case study highlights the ability of high-resolution, multispectral UAS-based imagery
523 to create accurate habitat and vegetation classification maps in brackish coastal marshes in
524 Louisiana. It also illustrates the ability of UAS-based vegetation classification maps to compare
525 site-wide vegetation communities among created and reference marsh sites in a manner not
526 logistically feasible using traditional plot-based sampling. Furthermore, we found that unlike
527 UAS-based surveys, the current, plot-based vegetation monitoring at the Lake Hermitage Marsh
528 Creation Project does not accurately represent site-wide vegetation cover at both created and
529 reference sites. Moreover, our case study illustrates the potential for UAS-based methods to

530 complement traditional plot-based sampling and aid restoration managers in optimizing the
531 number and placement of plots to reliably characterize vegetation communities and assess the
532 success of marsh creation projects intended to offset coastal land loss.

533 **5. ACKNOWLEDGEMENTS**

534 This paper is a result of research funded by the NOAA RESTORE Science Program and South
535 Central Climate Adaptation Sciences Center under award numbers NOAA-NOSNCCOS-2017-
536 2004875 and G21AC10678 (2022-09) respectively to the Louisiana State University, Louisiana
537 Universities Marine Consortium, Rutgers University, University of Wisconsin Madison, Michigan
538 Technological University, University of Tennessee-Knoxville, University of North Carolina
539 Charlotte, University of Louisiana Lafayette, University of Florida, and the University of South
540 Alabama. The funders had no role in the design, execution, or analyses of this project. Thank
541 you to Captain Zach's Myrtle Grove Properties LLC and the Bradish Johnson Trust for access to
542 their land. We also thank our project advisors (S. Brown, S. Osowski, J. Pahl, D. Richardi, K. Roy,
543 L.A. Sharp, R. Spears, P. Taylor, and P. Williams), technical monitors (M. Carle, S. Martin, and I.
544 Zink), program managers (F. Parker III and M. Langston) and Co-PIs (A. Engel, L. Hooper-Bùi, P.
545 López-Duarte, C. Martin, J. Olin, N. Rabalais, E. Swenson, and O. Jensen). Thank you to A. Stahl,
546 S. Wang, K. Loesser, S. Plaisance, G. Woods, C. Young, A. Davis for support in the field Bern
547 Wood and Adam Constantin and lab, E. D'sa and T. Quirk for advice on study design, and L.A.
548 Sharp, B. Wood and A. Constantin for constructive comments on an earlier version of this
549 manuscript. Data used in this study are publicly available via Dryad at
550 <https://doi.org/10.5061/dryad.3ffbg79vq>.

551 **WORKS CITED**

552 Abeysinghe, Tharindu, Anita Simic Milas, Kristin Arend, Breann Hohman, Patrick Reil, Andrew
553 Gregory, and Angélica Vázquez-Ortega. 2019. "Mapping Invasive Phragmites Australis in
554 the Old Woman Creek Estuary Using UAV Remote Sensing and Machine Learning
555 Classifiers." *Remote Sensing* 11 (11): 1380. <https://doi.org/10.3390/rs11111380>.

556 Anderson, Karen, and Kevin J Gaston. 2013. "Lightweight Unmanned Aerial Vehicles Will
557 Revolutionize Spatial Ecology." *Frontiers in Ecology and the Environment* 11 (3): 138–46.
558 <https://doi.org/10.1890/120150>.

559 Appeaning Addo, Kwasi, Philip-Neri Jayson-Quashigah, Samuel Nii Ardey Codjoe, and Francisca
560 Martey. 2018. "Drone as a Tool for Coastal Flood Monitoring in the Volta Delta, Ghana." *Geoenvironmental
561 Disasters* 5 (1): 17. <https://doi.org/10.1186/s40677-018-0108-2>.

562 Barlow, John, Jamie Gilham, and Ignacio Ibarra Cofrā. 2017. "Kinematic Analysis of Sea Cliff
563 Stability Using UAV Photogrammetry." *International Journal of Remote Sensing* 38 (8–
564 10): 2464–79. <https://doi.org/10.1080/01431161.2016.1275061>.

565 Barras, J., S. Beville, D. Britsch, S. Hartley, S. Hawes, J. Johnston, P. Kemp, et al. 2003. "Historic
566 and Projected Coastal Louisiana Land Changes: 1978–2050." USGS Open File Report 03–
567 334. Open-File Report. U.S. Geological Survey.

568 Brooks, Colin, Amanda Grimm, Amy M. Marcarelli, Nicholas P. Marion, Robert Shuchman, and
569 Michael Sayers. 2022. "Classification of Eurasian Watermilfoil (*Myriophyllum Spicatum*)
570 Using Drone-Enabled Multispectral Imagery Analysis." *Remote Sensing* 14 (10): 2336.
571 <https://doi.org/10.3390/rs14102336>.

572 Brooks, Colin N., Amanda G. Grimm, Amy M. Marcarelli, and Richard J. Dobson. 2019.
573 "Multiscale Collection and Analysis of Submerged Aquatic Vegetation Spectral Profiles
574 for Eurasian Watermilfoil Detection." *Journal of Applied Remote Sensing* 13 (03): 1.
575 <https://doi.org/10.1117/1.JRS.13.037501>.

576 Broussard, Whitney, Glenn Suir, and Jenneke Visser. 2018. "Unmanned Aircraft Systems (UAS)
577 and Satellite Imagery Collections in a Coastal Intermediate Marsh to Determine the
578 Land-Water Interface, Vegetation Types, and Normalized Difference Vegetation Index
579 (NDVI) Values." Engineer Research and Development Center (U.S.).
580 <https://doi.org/10.21079/11681/29517>.

581 Broussard, Whitney, Jenneke Visser, and Robert Brooks. 2020. "Quantifying Vegetation and
582 Landscape Metrics with Hyperspatial Unmanned Aircraft System Imagery in a Coastal
583 Oligohaline Marsh." *Estuaries and Coasts* 45 (4): 1058–69.
584 <https://doi.org/10.1007/s12237-020-00828-8>.

585 Cao, Jingjing, Wanchun Leng, Kai Liu, Lin Liu, Zhi He, and Yuanhui Zhu. 2018. "Object-Based
586 Mangrove Species Classification Using Unmanned Aerial Vehicle Hyperspectral Images
587 and Digital Surface Models." *Remote Sensing* 10 (1): 89.
588 <https://doi.org/10.3390/rs10010089>.

589 Chabot, Dominique, Christopher Dillon, Adam Shemrock, Nicholas Weissflog, and Eric P.S.
590 Sager. 2018. "An Object-Based Image Analysis Workflow for Monitoring Shallow-Water

591 Aquatic Vegetation in Multispectral Drone Imagery." *ISPRS International Journal of Geo-*
592 *Information* 7 (8). <https://doi.org/10.3390/ijgi7080294>.

593 Chabreck, Robert. 1970. "Marsh Zones and Vegetative Types in the Louisiana Coastal Marshes."
594 Doctor of Philosophy, Louisiana State University and Agricultural & Mechanical College.
595 https://doi.org/10.31390/gradschool_disstheses.1773.

596 Christie, Katherine S, Sophie L Gilbert, Casey L Brown, Michael Hatfield, and Leanne Hanson.
597 2016. "Unmanned Aircraft Systems in Wildlife Research: Current and Future
598 Applications of a Transformative Technology." *Frontiers in Ecology and the Environment*
599 14 (5): 241–51. <https://doi.org/10.1002/fee.1281>.

600 Congalton, Russell G. 1988. "A Comparison of Sampling Schemes Used in Generating Error
601 Matrices for Assessing the Accuracy of Maps Generated from Remotely Sensed Data." *PHOTOGRAMMETRIC ENGINEERING*.

602 Congalton, Russell G, and Kass Green. 2019. *Assessing the Accuracy of Remotely Sensed Data*.
603 3rd ed. Taylor and Francis Group, LLC. <https://doi.org/10.1201/9780429052729>.

604 Correll, Maureen D., Wouter Hantson, Thomas P. Hodgman, Brittany B. Cline, Chris S. Elphick,
605 W. Gregory Shriver, Elizabeth L. Tymkiw, and Brian J. Olsen. 2019. "Fine-Scale Mapping
606 of Coastal Plant Communities in the Northeastern USA." *Wetlands* 39 (1): 17–28.
607 <https://doi.org/10.1007/s13157-018-1028-3>.

608 Couvillion, Brady R., Michelle R. Fischer, Holly J. Beck, and William J. Sleavin. 2016. "Spatial
609 Configuration Trends in Coastal Louisiana from 1985 to 2010." *Wetlands* 36 (2): 347–59.
610 <https://doi.org/10.1007/s13157-016-0744-9>.

611 CPRA, Coastal Protection and Restoration Authority. 2023. "Louisiana's Comprehensive Master
612 Plan for a Sustainable Coast." *State of Louisiana*, May.

613 Cretini, Kari F., Jenneke M. Visser, Ken W. Krauss, and Gregory D. Steyer. 2011. "CRMS
614 Vegetation Analytical Team Framework-Methods for Collection, Development, and Use
615 of Vegetation Response Variables." Open-File Report 1097. Open-File Report. U.S.
616 Geological Survey.

617 DHNMP, Deepwater Horizon NRDA Monitoring Plan. 2015. "Lake Hermitage Marsh Creation -
618 NRDA Early Restoration Project."

619 DiGiacomo, Alexandra E., Ryan Giannelli, Brandon Puckett, Erik Smith, Justin T. Ridge, and Jenny
620 Davis. 2022. "Considerations and Tradeoffs of UAS-Based Coastal Wetland Monitoring in
621 the Southeastern United States." *Frontiers in Remote Sensing* 3 (August):924969.
622 <https://doi.org/10.3389/frsen.2022.924969>.

623 Doughty, Cheryl L., and Kyle C. Cavanaugh. 2019. "Mapping Coastal Wetland Biomass from High
624 Resolution Unmanned Aerial Vehicle (UAV) Imagery." *Remote Sensing* 11 (5): 540.
625 <https://doi.org/10.3390/rs11050540>.

626 Dronova, Iryna. 2015. "Object-Based Image Analysis in Wetland Research: A Review." *Remote
627 Sensing* 7 (5): 6380–6413. <https://doi.org/10.3390/rs70506380>.

628 Duo, Enrico, Arthur Chris Trembanis, Stephanie Dohner, Edoardo Grottoli, and Paolo Ciavola.
629 2018. "Local-Scale Post-Event Assessments with GPS and UAV-Based Quick-Response
630 Surveys: A Pilot Case from the Emilia–Romagna (Italy) Coast." *Natural Hazards and Earth
631 System Sciences* 18 (11): 2969–89. <https://doi.org/10.5194/nhess-18-2969-2018>.

632

633 DWHNRDAT, Deepwater Horizon Natural Resource Damage Assessment Trustees. 2017.
634 "Monitoring and Adaptive Management Procedures and Guidelines Manual Version
635 1.0." <http://www.gulfspillrestoration.noaa.gov/>.

636 Folse, Todd M, Thomas E McGinnis, Leigh A Sharp, Jonathan L West, Melissa K Hymel, John P
637 Troutman, Dona Weifenbach, et al. 2023. "A STANDARD OPERATING PROCEDURES
638 MANUAL FOR THE COASTWIDE REFERENCE MONITORING SYSTEM-WETLANDS AND THE
639 SYSTEM-WIDE ASSESSMENT AND MONITORING PROGRAM."

640 Forsmoo, Joel, Karen Anderson, Christopher J. A. Macleod, Mark E. Wilkinson, Leon DeBell, and
641 Richard E. Brazier. 2019. "Structure from Motion Photogrammetry in Ecology: Does the
642 Choice of Software Matter?" *Ecology and Evolution* 9 (23): 12964–79.
643 <https://doi.org/10.1002/ece3.5443>.

644 Hao, Mengyu, Wenli Zhao, Longjun Qin, Peng Mao, Xu Qiu, Lijie Xu, Yu Jiu Xiong, Yili Ran, and
645 GuoYu Qiu. 2021. "A Methodology to Determine the Optimal Quadrat Size for Desert
646 Vegetation Surveying Based on Unmanned Aerial Vehicle (UAV) RGB Photography."
647 *International Journal of Remote Sensing* 42 (1): 84–105.
648 <https://doi.org/10.1080/01431161.2020.1800123>.

649 Harris, J Mason. 2020. "Evaluating Coastal Wetland Restoration in Louisiana Using Drones."
650 University of Louisiana - Lafayette.

651 Hill, Troy D., and Brian J. Roberts. 2017. "Effects of Seasonality and Environmental Gradients on
652 *Spartina Alterniflora* Allometry and Primary Production." *Ecology and Evolution* 7 (22):
653 9676–88. <https://doi.org/10.1002/ece3.3494>.

654 Hoffmann, Samuel, Laura Steiner, Andreas H. Schweiger, Alessandro Chiarucci, and Carl
655 Beierkuhnlein. 2019. "Optimizing Sampling Effort and Information Content of
656 Biodiversity Surveys: A Case Study of Alpine Grassland." *Ecological Informatics* 51
657 (May):112–20. <https://doi.org/10.1016/j.ecoinf.2019.03.003>.

658 James-Pirri, Mary-Jane, Charles T. Roman, and James F. Heltshe. 2007. "Power Analysis to
659 Determine Sample Size for Monitoring Vegetation Change in Salt Marsh Habitats."
660 *Wetlands Ecology and Management* 15 (4): 335–45. <https://doi.org/10.1007/s11273-007-9034-x>.

662 Jaud, Marion, Christophe Delacourt, Nicolas Le Dantec, Pascal Allemand, Jérôme Ammann,
663 Philippe Grandjean, Henri Nouaille, et al. 2019. "Diachronic UAV Photogrammetry of a
664 Sandy Beach in Brittany (France) for a Long-Term Coastal Observatory." *ISPRS
665 International Journal of Geo-Information* 8 (6): 267.
666 <https://doi.org/10.3390/ijgi8060267>.

667 Keppeler, F.W., J.R. Junker, M.J. Shaw, S.B. Alford, A.S. Engel, L.M. Hooper-Bui, O.P. Jensen, et
668 al. 2023. "Can Created Saltmarshes Match Biodiversity of Pre-Existing Ones across
669 Scales? An Assessment from Microbes to Predators." *Exosphere* In Press.

670 Knight, Ian A., Blake E. Wilson, Madeline Gill, Leslie Aviles, James T. Cronin, John A. Nyman,
671 Scott A. Schneider, and Rodrigo Diaz. 2018. "Invasion of *Nipponaclerda Biwakoensis*
672 (Hemiptera: Aclerdidae) and *Phragmites Australis* Die-Back in Southern Louisiana, USA."
673 *Biological Invasions* 20 (10): 2739–44. <https://doi.org/10.1007/s10530-018-1749-5>.

674 LCWCRTF, Louisiana Coastal Wetlands Conservation and Restoration Task Force. 1993. "Coastal
675 Wetlands Planning, Protection, and Restoration Act." State of Louisiana.

676 Manfreda, Salvatore, Matthew McCabe, Pauline Miller, Richard Lucas, Victor Pajuelo Madrigal,
677 Giorgos Mallinis, Eyal Ben Dor, et al. 2018. "On the Use of Unmanned Aerial Systems for
678 Environmental Monitoring." *Remote Sensing* 10 (4): 641.
679 <https://doi.org/10.3390/rs10040641>.

680 Minchinton, Todd E., Hannah T. Shuttleworth, Justin A. Lathlean, Russell A. McWilliam, and
681 Trevor J. Daly. 2019. "Impacts of Cattle on the Vegetation Structure of Mangroves."
682 *Wetlands* 39 (5): 1119–27. <https://doi.org/10.1007/s13157-019-01143-0>.

683 Morgan, Grayson R., Daniel R. Morgan, Cuizhen Wang, Michael E. Hodgson, and Steven R. Schill.
684 2023. "The Dynamic Nature of Wrack: An Investigation into Wrack Movement and
685 Impacts on Coastal Marshes Using suAS." *Drones* 7 (8): 535.
686 <https://doi.org/10.3390/drones7080535>.

687 Pettorelli, Nathalie, Henrike Schulte To Bühne, Ayesha Tulloch, Grégoire Dubois, Cate Macinnis-
688 Ng, Ana M. Queirós, David A. Keith, et al. 2018. "Satellite Remote Sensing of Ecosystem
689 Functions: Opportunities, Challenges and Way Forward." Edited by Marcus Rowcliffe
690 and Mat Disney. *Remote Sensing in Ecology and Conservation* 4 (2): 71–93.
691 <https://doi.org/10.1002/rse2.59>.

692 R. Morgan, Grayson, Michael E. Hodgson, Cuizhen Wang, and Steven R. Schill. 2022.
693 "Unmanned Aerial Remote Sensing of Coastal Vegetation: A Review." *Annals of GIS* 28
694 (3): 385–99. <https://doi.org/10.1080/19475683.2022.2026476>.

695 Richardi, Danielle C. 2016. "Monitoring Plan for Lake Hermitage Marsh Creation (BA-42)."
696 Coastal Protection and Restoration Authority of Louisiana.

697 Steyer, Gregory D., Charles E. Sasser, Jenneke M. Visser, Erick M. Swenson, John A. Nyman, and
698 Richard C. Raynie. 2003. "A Proposed Coast-Wide Reference Monitoring System for
699 Evaluating Wetland Restoration Trajectories in Louisiana." In *Coastal Monitoring
700 through Partnerships*, edited by Brian D. Melzian, Virginia Engle, Malissa McAlister,
701 Shabeg Sandhu, and Lisa Kay Eads, 107–17. Dordrecht: Springer Netherlands.
702 https://doi.org/10.1007/978-94-017-0299-7_11.

703 Sturdivant, Emily, Erika Lentz, E. Robert Thieler, Amy Farris, Kathryn Weber, David Remsen,
704 Simon Miner, and Rachel Henderson. 2017. "UAS-SfM for Coastal Research: Geomorphic
705 Feature Extraction and Land Cover Classification from High-Resolution Elevation and
706 Optical Imagery." *Remote Sensing* 9 (10): 1020. <https://doi.org/10.3390/rs9101020>.

707 Trimble Inc. 2023. "eCognition Developer 10.3." Trimble Inc.
708 <https://geospatial.trimble.com/en/products/software/trimble-ecognition>.

709 Yang, Bo, Timothy L. Hawthorne, Hannah Torres, and Michael Feinman. 2019. "Using Object-
710 Oriented Classification for Coastal Management in the East Central Coast of Florida: A
711 Quantitative Comparison between UAV, Satellite, and Aerial Data." *Drones* 3 (3): 60.
712 <https://doi.org/10.3390/drones3030060>.

713

714 **Table 1.** Class area statistics for the habitat and vegetation classes found on each site
 715 calculated from UAS-based classification maps.

Site	Class	Area (ha)	Total area (%)	Land area (%)
LHA	Water	14.8	22.2	-
	Land	52	77.8	-
	Reeds	3.2	4.8	6.2
	Trees/Shrubs	1.3	1.9	2.5
	Grasses	40.6	60.8	78.1
	Rushes	6.9	10.3	13.3
LHB	Water	22.6	27.1	-
	Land	60.7	72.9	-
	Reeds	9.4	11.3	15.5
	Trees/Shrubs	4.4	5.3	7.2
	Grasses	45.3	54.4	74.6
	Rushes	1.6	1.9	2.6
LHC	Water	4.8	31	-
	Land	10.7	69	-
	Reeds	0.1	0.6	0.9
	Trees/Shrubs	0	-	-
	Grasses	9.7	62.6	90.7
	Rushes	0.9	5.8	8.4
CRMS-3680	Water	1.6	28.1	-
	Land	4.1	71.9	-
	Reeds	0	-	-
	Trees/Shrubs	0	-	-
	Grasses	4	70.2	97.6
	Rushes	0.1	1.8	2.4

716

717

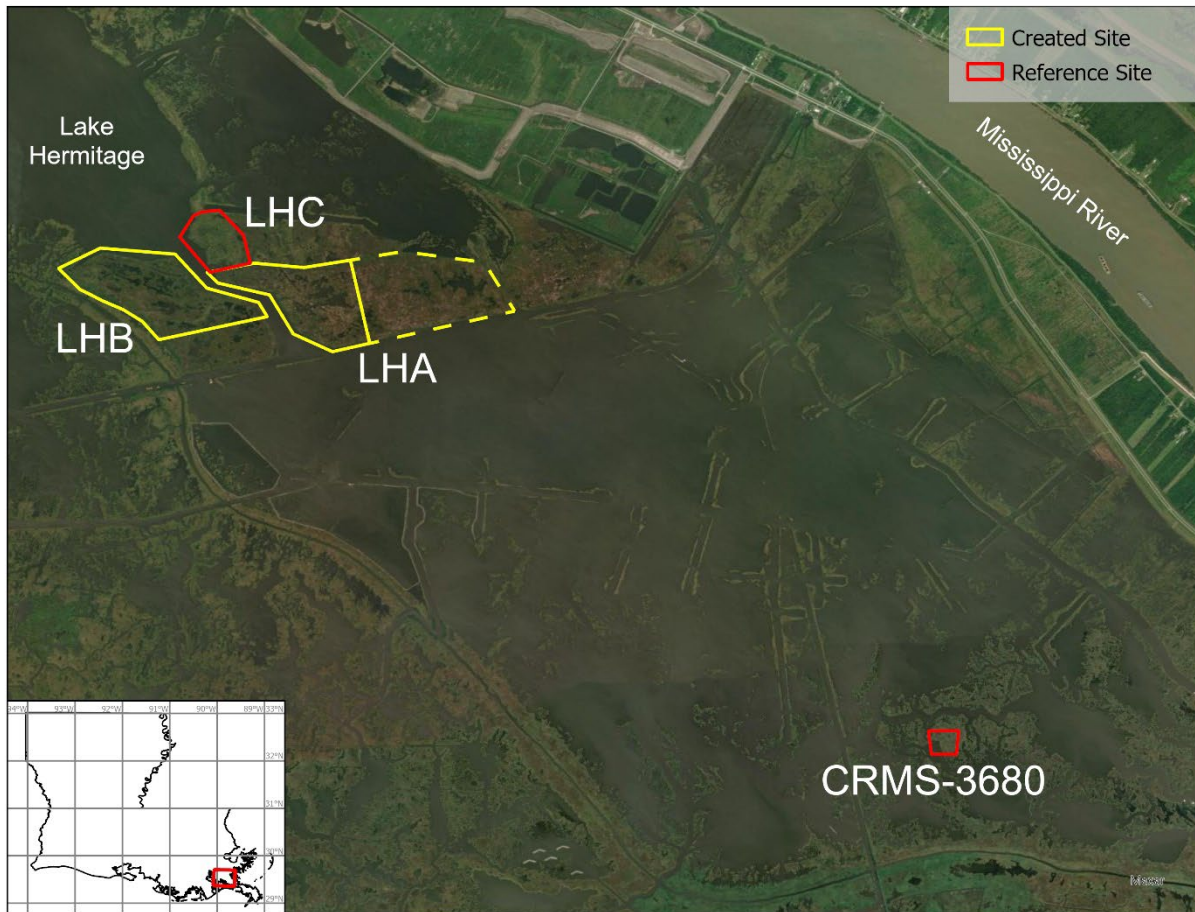
718 **Table 2.** The accuracy metrics of the imagery-based accuracy assessment performed for this
 719 project including Producer's, User's, and Total Accuracies. Producer's accuracy is a measure of
 720 errors of omission/false negatives for each habitat class. User's accuracy is a measure of errors
 721 of commission/false positives for each habitat class. Total accuracy describes how much of the
 722 target area/points were correctly classified by a classification map.

Site	Accuracy Metric	Habitat Classes (%)					Total
		Water	Shrubs/Trees	Reeds	Grasses	Rushes	
LHA	Producer's	70.4	83.3	77.8	91.7	44.1	-
	User's	80.9	100.0	70.0	77.3	68.2	-
	Total	-	-	-	-	-	77.9
LHB	Producer's	79.5	64.3	65.4	87.0	46.7	-
	User's	95.9	64.3	54.8	78.1	70.0	-
	Total	-	-	-	-	-	79.2
LHC	Producer's	75.0	-	80.0	89.7	85.7	-
	User's	100.0	-	80.0	83.9	60.0	-
	Total	-	-	-	-	-	83.3
CRMS-3680	Producer's	63.6	-	-	100.0	87.5	-
	User's	100.0	-	-	82.4	70.0	-
	Total	-	-	-	-	-	84.5

723

724 **Figure Captions**725 **Figure 1.** Location map of the four marsh areas used in this study. The dashed outline denotes
726 the eastern half of LHA that was not surveyed during this study due to logistical constraints.727 **Figure 2.** Detailed UAS workflow performed in this project. Bold text below each step indicates
728 the software used for each step of planning, processing, and analysis. Modified from Harris
729 (2020).730 **Figure 3.** UAS-derived habitat classification maps of the created (a,b) and reference (c,d) marsh
731 sites examined in this study.732 **Figure 4.** Vegetation class composition of each site using UAS data (a) and in-situ vegetation
733 composition (b,c) at both the class and taxa level. In-situ vegetation composition reflects
734 percent by biomass at LHA, LHB, and LHC and percent cover at CRMS-3680.735 **Figure 5.** Similarity analyses of created (blue) and reference (green) marsh sites vegetation
736 community composition at the class level using UAS (a) and in-situ (b) data.737 **Figure 6.** Power analysis with binomial regression curves indicating the probability of being
738 within 10% of the true of site-wide vegetation cover with increasing number of in-situ sampling
739 points (1-200 plots) at the created (a, b) and reference (b,c) marsh sites examined in this study.

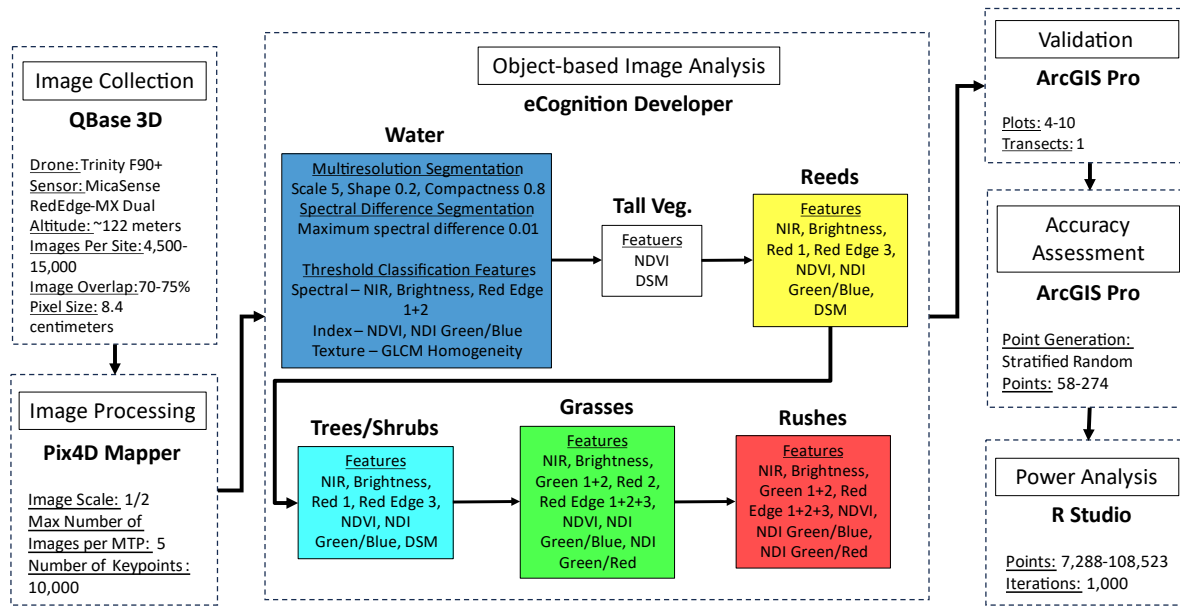
740



741

742 **Figure 1.** Location map of the four marsh areas used in this study. The dashed outline denotes the eastern half of
743 LHA that was not surveyed during this study due to logistical constraints.

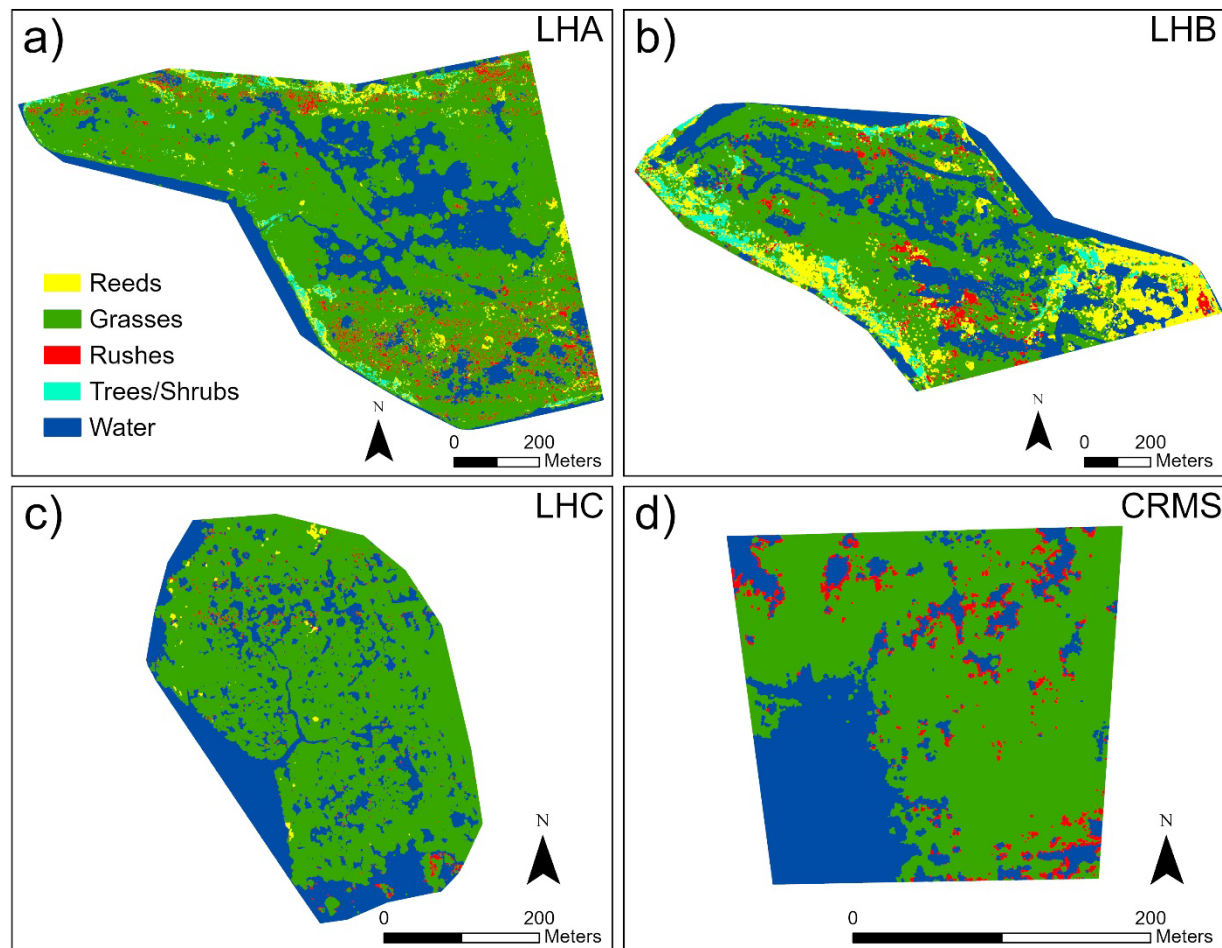
744



745

746 **Figure 2.** Detailed UAS workflow performed in this project. Bold text below each step indicates the software used
 747 for each step of planning, processing, and analysis. Modified from Harris (2020).

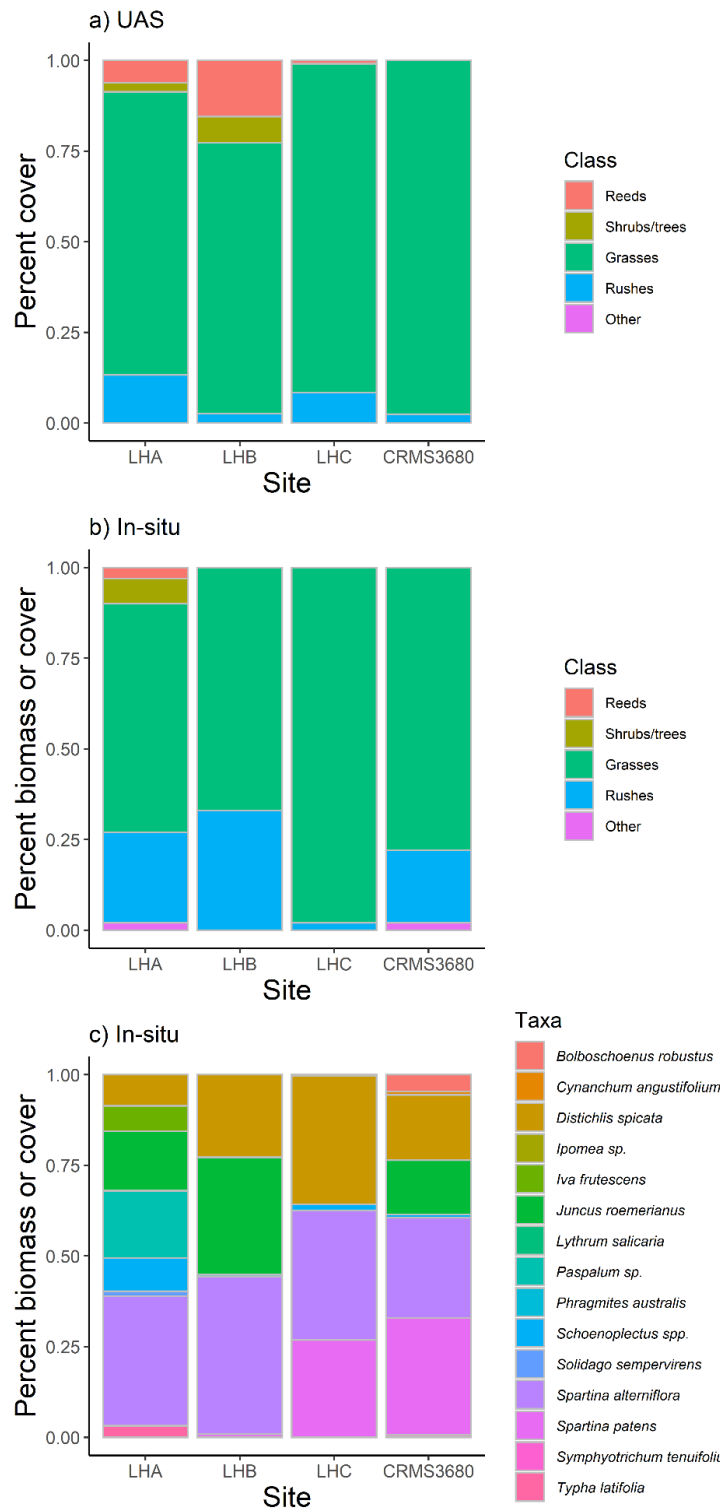
748



749

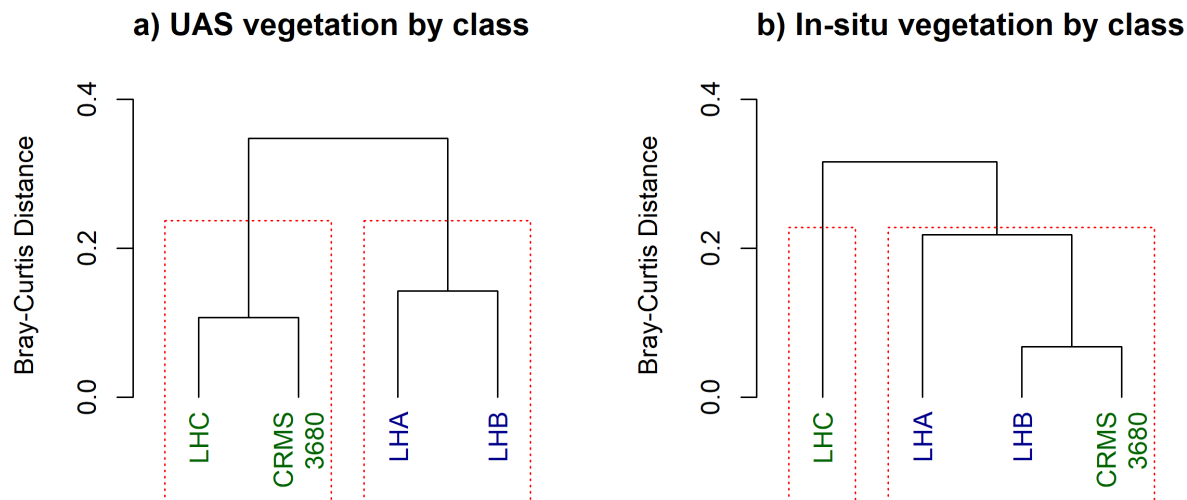
750 **Figure 3.** UAS-derived habitat classification maps of the created (a,b) and reference (c,d) marsh sites examined in
751 this study.

752



753

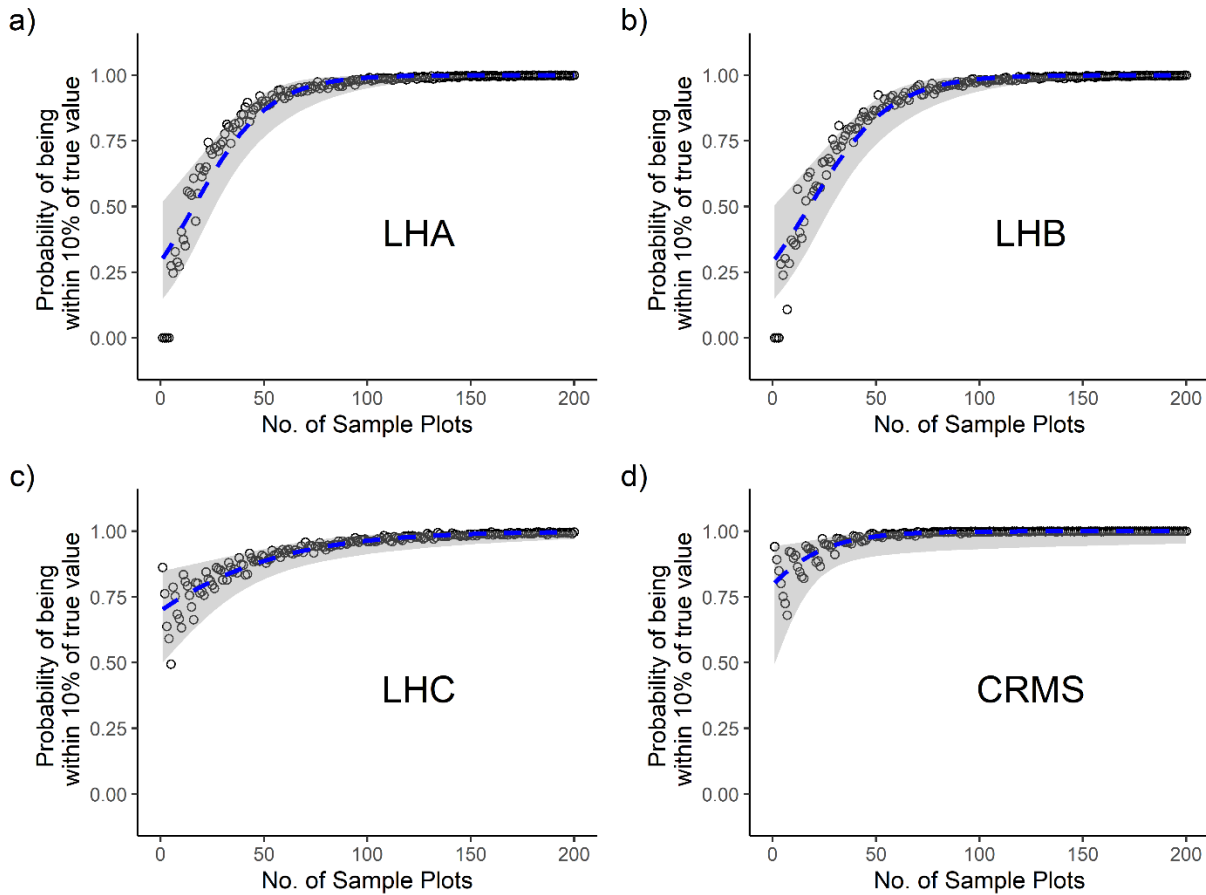
754 **Figure 4.** Vegetation class composition of each site using UAS data (a) and in-situ vegetation composition (b,c) at
 755 both the class and taxa level. In-situ vegetation composition reflects percent by biomass at LHA, LHB, and LHC and
 756 percent cover at CRMS-3680.



757

758 **Figure 5.** Similarity analyses of created (blue) and reference (green) marsh sites vegetation community composition
759 at the class level using UAS (a) and in-situ (b) data.

760



761

762 **Figure 6.** Power analysis with binomial regression curves indicating the probability of being within 10% of the true
 763 of site-wide vegetation cover with increasing number of in-situ sampling points (1-200 plots) at the created (a, b)
 764 and reference (b,c) marsh sites examined in this study.